Vortex Core Size in the Rotor Near-Wake

Larry A. Young
NASA Ames Research Center
Moffett Field, CA

Abstract

Using a kinetic energy conservation approach, a number of simple analytic expressions are derived for estimating the core size of tip vortices in the near-wake of rotors in hover and axial-flow flight. The influence of thrust, induced power losses, advance ratio, and vortex structure on rotor vortex core size is assessed. Experimental data from the literature are compared to the analytical results derived in this paper. In general, three conclusions can be drawn from the work in this paper. First, the greater the rotor thrust, the larger the vortex core size in the rotor near-wake. Second, the more efficient a rotor is with respect to induced power losses, the smaller the resulting vortex core size. Third, and lastly, vortex core size initially decreases for low axial-flow advance ratios, but for large advance ratios core size asymptotically increases to a nominal upper limit. Insights gained from this work should enable improved modeling of rotary-wing aerodynamics, as well as provide a framework for improved experimental investigations of rotor and advanced propeller wakes.

Nomenclature

A Rotor disk area, $A=\pi R^2$

b Fixed-wing semispan length, (m)

c Nominal blade chord length, (m)

C_{Pi} Induced power coefficient, $C_{Pi}=P_i/\rho A V_T^3$

C_P Rotor power coefficient, $C_P=P/\rho A V_T^3$

C_T Thrust coefficient, $C_T=T/\rho A V_T^2$

E Vortex filament kinetic energy per unit length, (N)

E_T Total kinetic energy of a vortex ring, (N-m)

k Induced power constant (Nondim.)

n Vortex tangential velocity profile parameter

N Number of rotor blades

P_i Rotor induced power, (N-m/sec)

r_c Vortex core radius, (m)

r_i Radii interpreted using flow visualization as vortex core size

R Rotor radius, (m)

T Rotor thrust, (N)

V Freestream velocity, (m/sec)

ν Inflow velocity through the rotor disk plane, (m/sec)

v_θ Vortex tangential velocity (m/sec)

V_T Tip Speed, (m/sec)

γ Vortex circulation strength, (m^2/sec)

λ Rotor inflow ratio, $\lambda=\nu/V_T$

μ_z Rotor axial-flow (or climb) advance ratio, $\mu_z=V/V_T$

ρ Atmospheric density, (kg/m^3)

σ Rotor solidity, $\sigma=Nc/\pi R$

θ Rotor collective (Deg.)

ψ_w Wake age (Deg.)

Introduction

Rotor vortex core size, and overall vortical structure, have a profound influence on rotor performance, noise, blade structural loads, and rotorcraft vibration. Community and passenger acceptance, safety, and economics of rotorcraft are dependent, in part, upon satisfactory and cost-effective solutions to these design and operational considerations. In turn, this requires that the estimation of rotor vortex structure and core size embody a more rigorous analytical or computational treatment than the trial-by-error or empirical approaches often used currently for rotorcraft. This paper will attempt to partially address this problem for rotors in hover and climb.

Prandtl employed a conservation of kinetic energy approach to derive an analytical relation between trailed vortex core size and a fixed-wing's semispan length (Ref. 1). Prandtl's analysis assumed an elliptic loading for the fixed-wing and that, further, the trailed tip vortex structure was a Rankine line vortex. The result was a fixed-wing vortex core size expression of r_c=0.171b (where b is the wing semispan length). Later authors including Betz, Kayden, and Pullin (Ref. 2) proposed alternate analytical expressions for vortex core size for fixed-wing aircraft by modeling the vortex sheet roll-up process. The work on rotary-wing aircraft for vortex core size estimation, on the other hand, is limited and predominately empirical in nature.

This paper will employ a conservation of kinetic energy approach (an analogous methodology to that applied in the Prandtl fixed-wing solution) to derive a first-order set of vortex core size analytical expressions for rotorcraft. The derived analytical expressions will be limited to tip vortex core size estimates in the rotor near-wake.

The rotor "near-wake" can be defined in number of ways. It can represent a nominal completion of the vortex sheet roll-up process. It can describe reaching a certain cut-off limit in wake contraction or

rotor slipstream acceleration. It can be defined in terms of the first blade passage. It can be defined in terms of a certain convection distance downstream of the disk plane. Or, it can be defined in terms of certain wake age, ψ_W, limit. As discussed in Refs. 3-4 -- or, alternatively, Refs. 5-6 -- rotary-wing trailed vortex filaments have time-dependent behavior in the mid- to far-wake regions of the rotor slipstream where vortex circulation and core size change with wake age or time. The kinetic energy of the rotor vortices is conserved (the theoretical underpinning of the analysis in this paper) only in the near-wake, prior to the onset of vortex filament decay, or wake evolution. Therefore, definition of the near-wake in terms of a wake age limit is important. The near-wake will be assumed in this paper to be generally within the range of $5 < \psi_W < 125$ degrees -- i.e., after completion of vortex sheet roll-up but before vortex filament decay begins.

Review and Assessment of Experimental Results from the Literature

Several authors (for example, Refs. 6 – 18 for hover, and Refs. 19 – 24 for axial-flow flight) have attempted to either directly measure rotor vortex core size via various velocimetry techniques or indirectly estimate core size through interpretation of flow visualization results. A wide variety of rotor configurations have been studied: from single-bladed, untwisted, rectangular planform rotors all the way to multi-bladed, advanced propellers with large amounts of twist, taper, and sweep. A wide spectrum of operating conditions have also been studied: small-scale rotors operating at low tip Reynolds and Mach numbers with low disk loading, to full-scale rotors at moderate to high Reynolds and Mach numbers at high disk loading. Finally, several different experimental techniques have been used to study the near-wake rotor trailed tip vortex structure: laser light sheet smoke flow visualization, wide-field shadowgraphy, hot-wire anemometry, particle image velocimetry (PIV), and laser-doppler velocimetry (LDV), among others. In many cases, in fact, the primary emphasis has been on the development and demonstration of the experimental technique being employed and less on the rotor configuration and operating condition being used as the test case. All of the above factors have made it extremely difficult to gain a

comprehensive, rigorous understanding of the rotor trailed vortical structures (including tip vortex core size) as influenced by rotor characteristics and operating conditions.

It should also be noted that interpretation of flow visualization results for estimating vortex core size can be fraught with potential errors. To discuss this issue further it is necessary to make the distinction between r_c, the vortex core size measured via velocimetry techniques, and r_i, a vortex "image" radii interpreted using various flow visualization technologies as being the vortex core size. (The measurement r_i is sometimes known as a "particle void" for some smoke flow visualization results and the "outer core" as seen in wide-field shadowgraphy results.) Generally, for very small values of wake age, as $\psi_w \to 0$, the vortex core size and an image radius can be considered approximately equal (to the first-order, at least), i.e. $r_c \approx r_i$. However, as $\psi_w \to \infty$, then generally there are substantial differences between the two measurements (by a factor of two/three or greater), i.e. $r_c \neq r_i$. Thus flow visualization techniques can be used to gain a first-order sense of the vortex core size for the rotor near-wake, but provides completely unacceptable results for the rotor mid- and far-wakes.

Without making any prejudgments as to measurement accuracy and the relative merits of the experimental techniques employed, it is hoped that examining data (Refs. 5-24) from the literature will yield insights into vortex core size trends that relying on the individual study results can not. Tables 1 and 2 summarize some key details from the individual literature studies, for the hover and axial-flow conditions, respectively. Figure 1 presents vortex core size measurements from various different sources. Because of the wide spectrum of experimental techniques employed (and their accuracy), the diverse rotor configurations tested, and the necessary inference/estimation of rotor operating conditions in some cases, the vortex core size trend noted in Fig. 1 can be considered only qualitative, but highly illuminating, in nature. (As a point of information, an alternate analysis of rotor vortex trends based upon a survey of experimental data from the literature can be found in Ref. 25. This analysis focuses on blade geometry and Reynolds number scaling effects on rotor vortex properties, principally observed trailed vortex strength relative to maximum rotor bound circulation.)

Table 1 – Near-Wake Hover Vortex Core Size Measurements

Ref.	Exp. Tech.	Rotor Description	Data Reduction/Analysis
Cook	Hot-Wire	Single-bladed rotor; NACA 0012 blade airfoil; $\sigma \approx 0.016$; $M_{Tip}=0.54$	Thrust & r_c given
Heineck	3-D PIV	Same rotor as McAlister; two-bladed, untwisted, rectangular planform rotor	Thrust, Power, & r_c (at wake age = 210 Deg.) given
Han	3-D LDV	Single-bladed, untwisted, rectangular planform rotor; NACA 2415 blade airfoil; $M_{Tip}=0.29$ & $Re_{Tip}=250{,}000$	C_T & r_c given
Martin	3-D LDV	Single-bladed untwisted rotor; NACA 2415 airfoil; $\sigma \approx 0.035$; different tip shapes studied	C_T & r_c given; measurements for different wake ages
McAlister (2001)	LDV	Two-bladed untwisted, rectangular planform rotor; rotor; NACA 0012 airfoil outer 50% span & linear transition to NACA 0020 for inboard 50%	C_T , C_P, & r_c given
Muller	"Flow Visualization Gun" (Burning Tungsten projectile pellets)	Two-bladed rotor; 33 Deg. twist; $\theta=10$ Deg.; "rotor in a box," i.e. ceiling/floor & walls less than 2R from rotor blade tips; $M_{Tip}=0.14$	C_T & γ estimated by knowing max vortex tangential velocity, & core size, & assuming Scully vortex
Pouradier	2-D LDV	Three-bladed, rectangular planform rotor; -12.1 Deg. linear twist; Aerospatiale SA 13106, 13109, & 13112 (12% thick)	C_T/σ and C_Q/σ given; core size estimated from reported vortex tangential velocity profiles
Seelhorst	3-D LDV	Four-bladed untwisted rotor; $\sigma \approx 0.135$; NACA 0015 blade airfoil; $\theta=15$ Deg.; wake induced velocity = 7m/sec.	C_T "range" estimated based on induced/convection velocity measurement of vortex & using k=1 to k=1.2
Swanson	Wide-Field Shadowgraphy	Three-bladed 7/38-scale "JVX" tiltrotor proprotor; -34 Deg. twist; $\sigma \approx 0.1144$; $M_{Tip}=0.69$; XN-09, -12, -18, & -28 airfoils	Range of C_T, C_P, and r_c ("outer core" image) values; k estimated from thrust/power polar
Thompson	Laser Sheet Smoke flow visualization and 3-D LDV	Single-bladed, untwisted, rectangular planform rotor; NACA 0012 blade airfoil; $M_{Tip}=0.094$ & $Re_{Tip}=269{,}000$	C_T & r_c given
University of Maryland	Shadowgraph	Four-bladed rectangular planform rotor; -13 Deg. twist; RC(3)10 & RC(4)10 blade airfoils	C_T, C_P, & r_c given

It should be noted that most of the Refs. 19-24 axial-flow data has been derived from advanced propeller studies for high-speed subsonic flight. In many cases a vortex core size estimate had to be gleaned from published vortex velocity time histories rather than being directly noted in the study itself. This is noted in Table 2. Further, in some cases, key rotor operating conditions had to be inferred from available information in the individual study reports. This is noted in both Tables 1 and 2.

Table 2 – Near-Wake Axial-Flow Vortex Core Size Measurements

Ref.	μ_z	Exp. Tech.	Rotor Description	Data Reduction/Analysis
Deppe	0.05	Ultrasonic anemometer	Two-bladed, tapered wind turbine operating as propeller; blade lift mismatch with two different resultant core sizes cited	Power, γ, & r_c given for each rotor blade tip vortex; Thrust & C_T inferred.
Hanson	0.28	Hot-Wire	SR-3 (Two-bladed) Adv. Propeller; helical tip Mach # = 1.17	Wake velocity measurements reported; regression analysis using Scully profile performed & r_c, γ, and C_T estimated using tangential velocities
Querin	0.04 & 0.08	Smoke flow visualization	Four-bladed, untwisted, untapered rotor; NACA 0012 blade airfoils; $\sigma \approx 0.154$; θ=10 Deg.; $Re_{Tip} \approx$ 129,000 & 172,000	"Particle void" core sizes given; motor power max rating cited; linear power relationship assumed for specified operating conditions; Thrust inferred from power estimate
Lavrich	0.29	Hot-Wire	Three-bladed (single) CR-9 Adv. Propeller at simulated take-off condition; θ=35 Deg.	Power, Thrust, & r_c given; wake velocities provided
McAlister (2002)	0.005	PIV	Two-bladed 1/7-scale OLS rotor, axial-flow configuration in 7x10 settling chamber	Wake age survey measuring wake vorticity and velocities with estimates for r_c, γ, and particle "void" size for one C_T and collective condition
Tillman	0.91	Hot-Wire	(Single) five-bladed CRXP-1 Adv. Propeller	Wake velocity measurements reported; regression analysis using Scully profile performed & r_c, γ, and C_T estimated using tangential velocities

The data shown in Fig. 1 collapses surprisingly well onto a single curve for the $ln(r_C/R)$ versus $1/\sqrt{C_T}$ trend, with the exception perhaps of one or two outlying points. Thompson (Ref. 9) cites three different data points: two points using smoke visualization of the vortex particle void and a LDV measurement of core size. The Ref. 9 LDV core size measurement is the principal outlying point shown in Fig. 1. Smearing of the vortex core velocity profiles - because of the ensemble averaging techniques used in the Ref. 9 LDV work - could be the reason for the overly large estimate of the vortex core size. This apparent functional dependence of $ln(r_C/R)$ with respect to $1/\sqrt{C_T}$ is not coincidental, as will be discussed in the analytical treatment later in the paper.

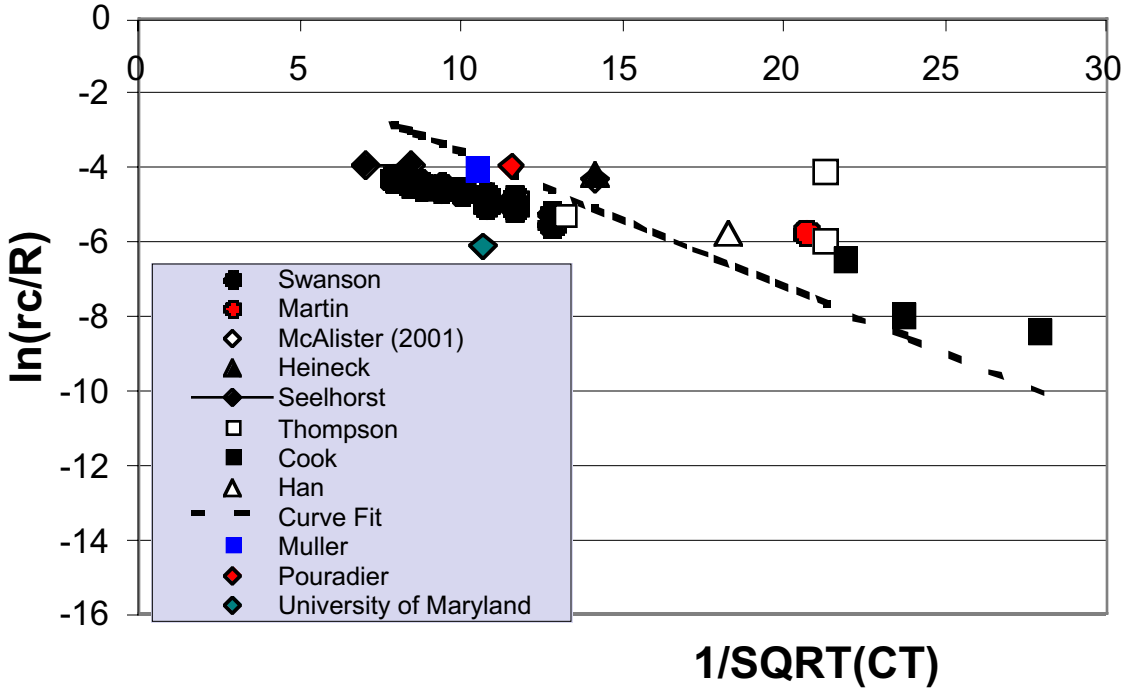

Fig. 1 – Rotor Hover Near-Wake Vortex Core Size Trend (Experimental Data from the Literature)

Vortex Core Size as Influenced by Rotor Thrust and Induced Power

In this study, the overall rotor induced power is assumed equal to the trailed vortex filament kinetic energy, as seen in Eq. 1. This equation is the kinetic energy conservation law applied to a rotor and its trailed tip vortices.

$$P_i = NEV_T \qquad (1)$$

P_i is the rotor induced power. The rotor induced power is equal to the product of the number of blades (and the number of trailed tip vortices), N, the kinetic energy per unit length of each trailed rotor tip vortex, E, and the rotor tip speed, V_T. The rotor induced power is also given by momentum theory. The key to the application of Eq. 1 is the definition of a suitable vortex model for the wake -- and the associated kinetic energy estimate -- of a rotor in hover or axial-flight (climb).

Deriving a kinetic energy expression for the helical vortex filaments of a rotor is not analytically tractable. Vortex rings, on the other hand, have been used previously in the literature to model axisymmetric rotor wakes (Ref. 4) and have simple analytic expressions for induced velocity and kinetic energy. For first-order analytical estimates of near-wake vortex core size, the use of vortex rings to model the rotor wake is often an acceptable and convenient compromise.

The analysis presented in this paper does not actually require modeling the complete rotor wake with a semi-infinite and regularly spaced vortex rings. Instead, the key modeling argument of this paper is the hypothesis that the rotor tip vortices trailed *per unit time* can be represented with reasonable accuracy by small segments, or arcs, of a vortex ring instead of helical curved elements (Fig. 2). This approximation has more validity for lightly loaded rotors than those with high disk loading. This is because the helical pitch angles of the rotor vortex filaments are proportional to rotor thrust.

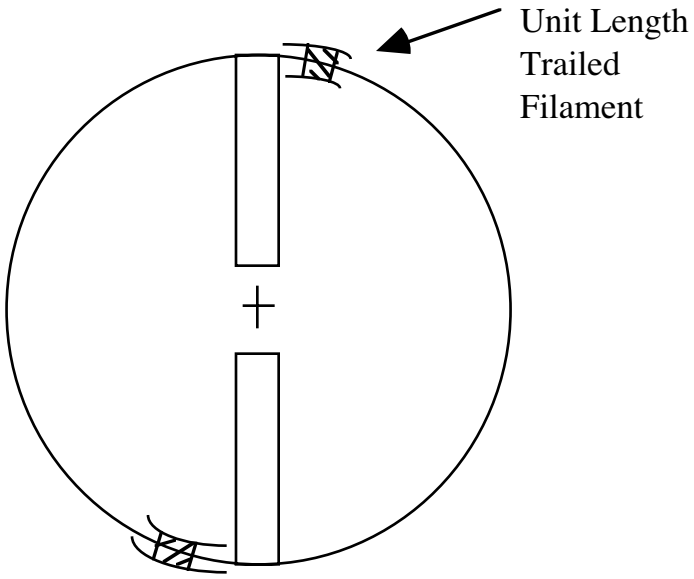

Fig. 2 - Vortex Filaments Trailed Per Unit Time As Represented By Vortex Ring Segments/Arcs (Planform View of Rotor)

Kinetic energy expressions for vortex rings (assuming various forms of finite-cores) can be found in the literature or readily derived. Reference 26 summarizes the derivation of a kinetic energy expression for a vortex ring having a uniform core (Eq. 2).

$$E_T = \frac{\rho\gamma^2 R}{2}\left\{\ln\left(\frac{8R}{r_c}\right) - \frac{7}{4}\right\} \qquad (2)$$

A vortex ring having a uniform core has a core with a constant rate of angular rotation. This is analogous to the two-dimensional Rankine vortex. Given Eq. 2, Eq. 3 directly follows, wherein the kinetic energy per unit length of one of N (Rankine) vortex ring segments can be found.

$$E = \frac{\rho\gamma^2}{4\pi N}\left\{\ln\left(\frac{8R}{r_c}\right) - \frac{7}{4}\right\} \qquad (3)$$

Equation 3 can now be substituted into Eq. 1 and solving for r_c/R gives.

$$r_c/R = 8e^{-\left\{\frac{7}{4}+\frac{4\pi}{\rho\gamma^2}\frac{P_i}{V_T}\right\}} \tag{4}$$

From momentum theory, the rotor induced power (Refs. 27 and 28, for example) is

$$P_i = T(V+v) \tag{5a}$$

and where the induced inflow velocity through the rotor disk is

$$v = -\frac{V}{2} + \sqrt{\left(\frac{V}{2}\right)^2 + \frac{C_T}{2}k^2V_T^2} \tag{5b}$$

The induced power or inflow correction factor, k, is generally empirically defined. For ideal induced power, k=1.

From classic rotor vortex theory (Ref. 28), the trailed circulation is

$$\gamma = \frac{4\pi Rv}{V_T}(V+v) \tag{6}$$

Substituting Eqs. 5a-b and 6 into Eq. 4 and simplifying gives the following non-dimensional expression for vortex core size (Eq. 7).

$$r_c/R = 8e^{-\frac{1}{4}\left\{7+\frac{C_T}{\lambda^2(\mu_z+\lambda)}\right\}} \tag{7a}$$

Or

$$\ln\left(r_c/R\right) = \ln 8 - \frac{1}{4}\left\{7 + \frac{C_T}{\lambda^2\left(\mu_z + \lambda\right)}\right\} \qquad (7b)$$

Where the mean rotor inflow, λ, is given by $\lambda \equiv v/\Omega R = v/V_T$ and the axial-flow advance-ratio, μ_z, is given by $\mu_z = V/V_T$. Correspondingly, the induced power constant, k, for hover is used to estimate the induced power coefficient and the rotor inflow.

$$C_{Pi} = k\sqrt{\frac{C_T^3}{2}} \qquad (8)$$

$$\lambda = k\sqrt{\frac{C_T}{2}} \qquad (9)$$

For hover (μ_z=0), substituting in the above expression for rotor wake mean inflow, λ, the relationship between vortex core size and rotor thrust is

$$\ln\left(r_c/R\right) = \frac{a}{\sqrt{C_T}} + b \qquad (10)$$

where a and b are constants. This linear vortex core size to rotor thrust relationship, Eq. 10, is consistent with the experimental trend observed in Fig. 1. Figure 3 provides a more detailed examination of the experimental data as compared to the predictions from Eq. 7 (and, later, results from Eq. 17a for a Scully-type vortex). A family of curves of different values of induced power constants is provided in Fig. 3. As can be readily seen the vortex core size is dependent upon the induced power losses, as represented by the induced power constant, k, and the vortex velocity profile/structure. This will be discussed in more detail later in the paper. Also to be examined is the influence of axial-flow advance-ratio on the rotor vortex core size.

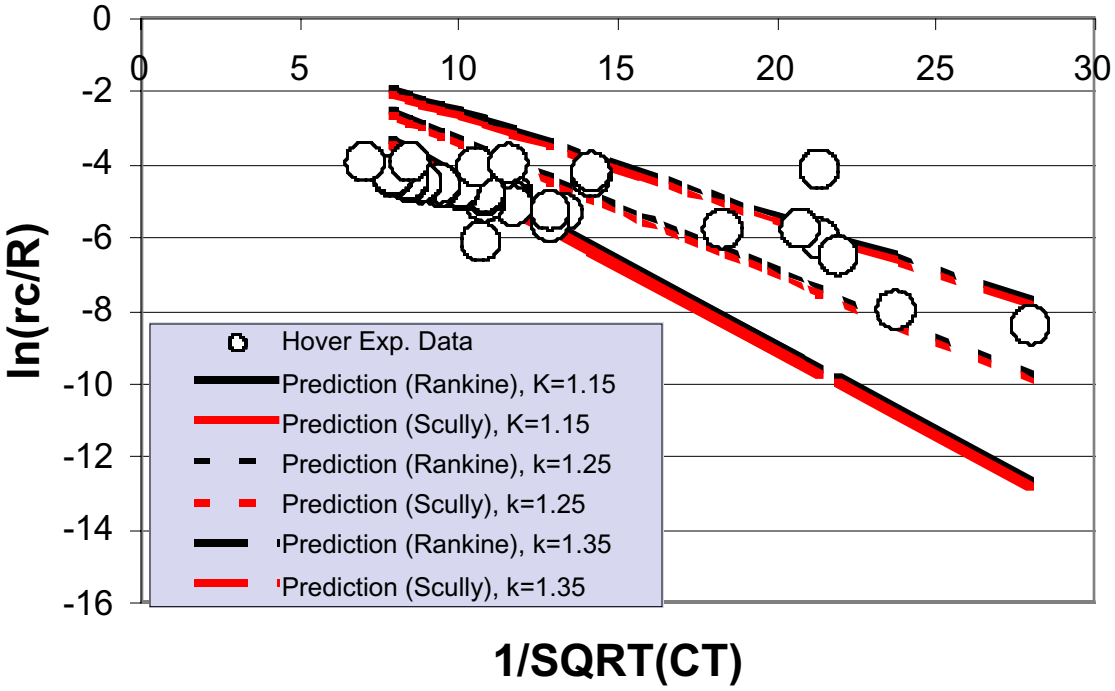

Fig. 3 – Correlation of Predictions with Experimental Data

Figure 3 results can be compared to the well-known, empirical recommendation from Scully for vortex core size, i.e., r_C=0.0025R or, rather, in this case $ln(r_c/R)$ = -5.99 (Ref. 28). A few authors have previously suggested, based on limited experimental observations, that rotor thrust may affect vortex core size. However, none of the generally accepted empirical "rules of thumb" -- including the Scully recommendation -- account for this effect. This is perhaps the most important aspect of Eq. 7.

Equation 7 also predicts the effect of axial-flow flight advance ratio on core size. Increasing the advance ratio (or climb speed) reduces the vortex core size, as per the Eq. 7 predictions. This is a largely unexplored research area for rotorcraft. Very limited experimental data exists for vortex core size for rotors, or propellers, in axial-flow flight. Clearly, the asymptotic limit with respect to increasing advance ratio of Eq. 7 is physically unrealistic: the vortex core size can not become infinitesimally small as $\mu_z \to \infty$. Instead, perhaps, the $\mu_z \to \infty$ asymptotic limit should approach the Prandtl fixed-wing core size estimate (i.e., $r_c/R \to 0.171$). It would seem sensible to expect that the trend of decreasing vortex core size with advance ratio as

predicted by Eq. 7 would at some point be reversed. This will be discussed in more detail later in the paper.

The analytical methodology that led to the derivation of Eq. 7 will now be extended to different types of assumed rotor trailed tip vortex structure.

Influence of Vortex Structure on Core Size

Several models have been proposed to describe the vortical structure of rotor vortices. The objective of the discussion in this section is not to advocate or justify the viability of one model of rotor vortex structure over another. Instead, the influence of vortex structure on vortex core size will be examined. It will be found the vortex structure affects from a small to modest degree the vortex core size. In order to accomplish this demonstration it will be necessary to employ more generalized expressions for vortex kinetic energy and velocity profiles than the expressions (Rankine/uniform-core) so far used.

From Ref. 2, for a vortex ring of arbitrary tangential velocity distribution, v_θ, the kinetic energy per unit length of a vortex ring is given by Eq. 11.

$$E \approx \frac{\rho\gamma^2}{4\pi}\left[\ln\left(\frac{8R}{r_c}\right) - 2 + \left(\frac{2\pi}{\gamma}\right)^2 \int_0^{r_c} v_\theta^2 r dr\right] \qquad (11)$$

In Eq. 11, and the following discussion in this section, r is a local radial coordinate with respect to the vortex center. This local radial coordinate describes the vortex tangential velocity profile. For a uniform core vortex, where $v_\theta = \gamma r/2\pi r_c^2$ for $r<r_c$, Eq. 11 reduces to Eq. 3.

Vatistas (Ref. 6) derived a general expression that encompasses a series of tangential velocity profiles for vortex structure. Alternate kinetic energy and vortex core size expressions will now be derived

based on the Vatistas vortex model. The new vortex core size predictions will be compared to the earlier results noted in this paper for a uniform, or Rankine, vortex model.

The tangential velocity profile of a Vatistas vortex is given by the expression:

$$v_\theta = \frac{\gamma r}{2\pi\left(r_c^{2n} + r^{2n}\right)^{1/n}} \qquad (12)$$

where n is an arbitrary integer and r is the local radial coordinate for the vortex tangential velocity profile.

The Vatistas vortex model, Eq. 12, as discussed in Ref. 6, is a generalization of several well-known vortex velocity profiles. When n=1, then the Scully vortex profile model (Ref. 28) is reproduced. Correspondingly, when n=2, then the Vatistas model gives the Bagai-Leishman vortex profile model (Ref. 6). Finally as $n \to \infty$, then the Vatistas model reduces to a Rankine vortex velocity profile.

Substituting Eq. 12 into 11 yields a kinetic energy expression for vortex profiles based on the Vatistas model.

$$E \approx \frac{\rho\gamma^2}{4\pi}\left[\ln\left(\frac{8R}{r_c}\right) - 2 + \int_0^{r_c} \frac{r^3}{\left(r_c^{2n} + r^{2n}\right)^{2/n}} dr\right] \qquad (13)$$

Making the integration substitutions

$$x = r^{2n} \qquad r = x^{1/2n} \qquad dr = \frac{1}{2n} x^{\frac{1}{2n}-1} dx \qquad (14a\text{-}c)$$

Equation 13 becomes

$$E \approx \frac{\rho\gamma^2}{4\pi}\left[\ln\left(\frac{8R}{r_c}\right) - 2 + \frac{1}{2n}\int \frac{x^{2/n-1}}{\left(r_c^{2n}+x\right)^{2/n}}dx\right] \qquad (15)$$

For n=1 or 2, 2/n is an integer, and integral formulas from standard handbooks can be employed to complete the following analytical derivations for the vortex kinetic energy per unit length for the two well-known vortex structure models:

$$\begin{aligned} E &\approx \frac{\rho\gamma^2}{4\pi}\left[\ln\left(\frac{8R}{r_c}\right) - 2 + \frac{1}{2}\int \frac{x}{\left(r_c^2+x\right)^2}dx\right] \\ &\approx \frac{\rho\gamma^2}{4\pi}\left[\ln\left(\frac{8R}{r_c}\right) - 2 + \frac{1}{2}\left[\ln\left(r_c^2+r^2\right) + \frac{r_c^2}{r_c^2+r^2}\right]\Bigg|_0^{r_c}\right] \qquad \text{(for n=1)} \qquad (16a) \\ &\approx \frac{\rho\gamma^2}{4\pi}\left[\ln\left(\frac{8R}{r_c}\right) - \frac{9}{4} + \frac{1}{2}\ln 2\right] \end{aligned}$$

$$\begin{aligned} E &\approx \frac{\rho\gamma^2}{4\pi}\left[\ln\left(\frac{8R}{r_c}\right) - 2 + \frac{1}{4}\int \frac{dx}{\left(r_c^4+x\right)}\right] \\ &\approx \frac{\rho\gamma^2}{4\pi}\left[\ln\left(\frac{8R}{r_c}\right) - 2 + \frac{1}{4}\ln\left(r_c^4+r^4\right)\Big|_0^{r_c}\right] \qquad \text{(for n=2)} \qquad (16b) \\ &\approx \frac{\rho\gamma^2}{4\pi}\left[\ln\left(\frac{8R}{r_c}\right) - 2 + \frac{1}{4}\ln 2\right] \end{aligned}$$

Substituting Eqs. 16a-b into Eqs. 1, 5a-b, and 6 yields the following expressions for vortex core size for the n=1 and n=2 vortex structure models.

$$\ln\left(r_c/R\right) = \ln 8 - \frac{1}{4}\left\{9 - 2\ln 2 + \frac{C_T}{\lambda^2\left(\mu_z+\lambda\right)}\right\} \qquad \text{(for n=1)} \qquad (17a)$$

$$\ln\left(r_c/R\right) = \ln 8 - \frac{1}{4}\left\{8 - \ln 2 + \frac{C_T}{\lambda^2\left(\mu_z + \lambda\right)}\right\} \qquad \text{(for n=2)} \qquad (17b)$$

Figure 4 is a comparison of the Refs. 6-18 data with the new predictions. Equation 7, and alternatively Eqs. 17a-b, as noted before capture the general trend of the experimental data.

The compilation of experimental data in Fig. 1 -- and the analytical work of this paper as represented by Eqs. 7 and 17a-b and Figs. 3 and 4 -- are compelling demonstrations of the influence of rotor thrust and induced power on vortex core size.

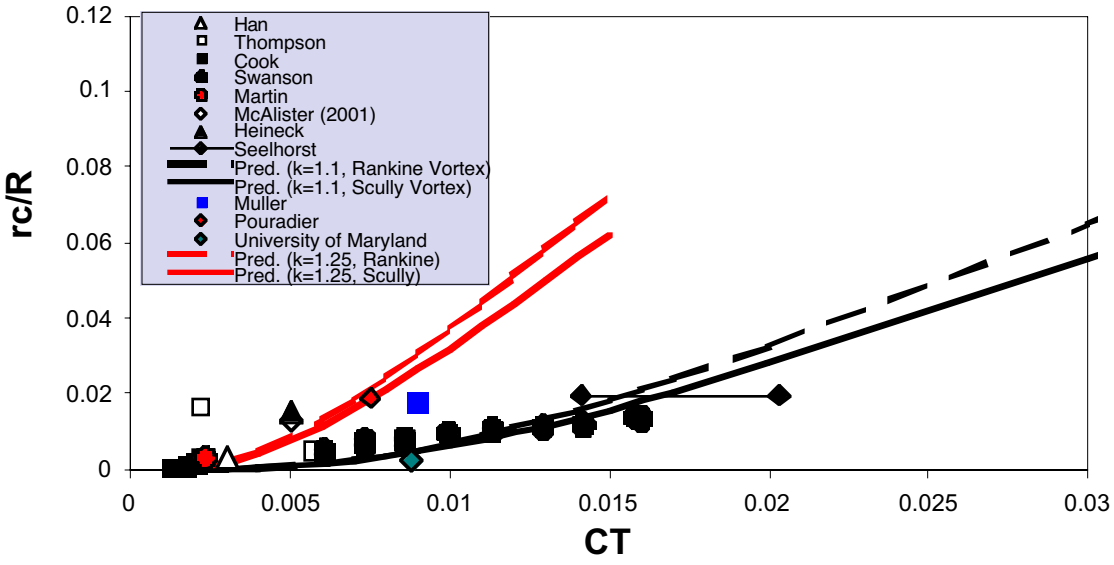

Fig. 4 – Core Size as a Function of Thrust Coefficient for Two Different Assumed Vortex Structures (Scully versus Rankine Vortices)

Figure 5 shows the predicted influence of vortex structure on core size using Eqs. 7 and 17a-b (assuming, in this case, k=1). As the parameter n increases, the core size also increases. However, vortex structure is clearly not a major driver in the determination of vortex core size. Induced power losses, and overall rotor efficiency, have more impact on core size than does vortex structure. This is actually a relatively positive outcome with regards to the application of the results of this paper. An accurate analytical/computational

representation of the velocity profiles for rotor vortices is still an active area for rotorcraft research.

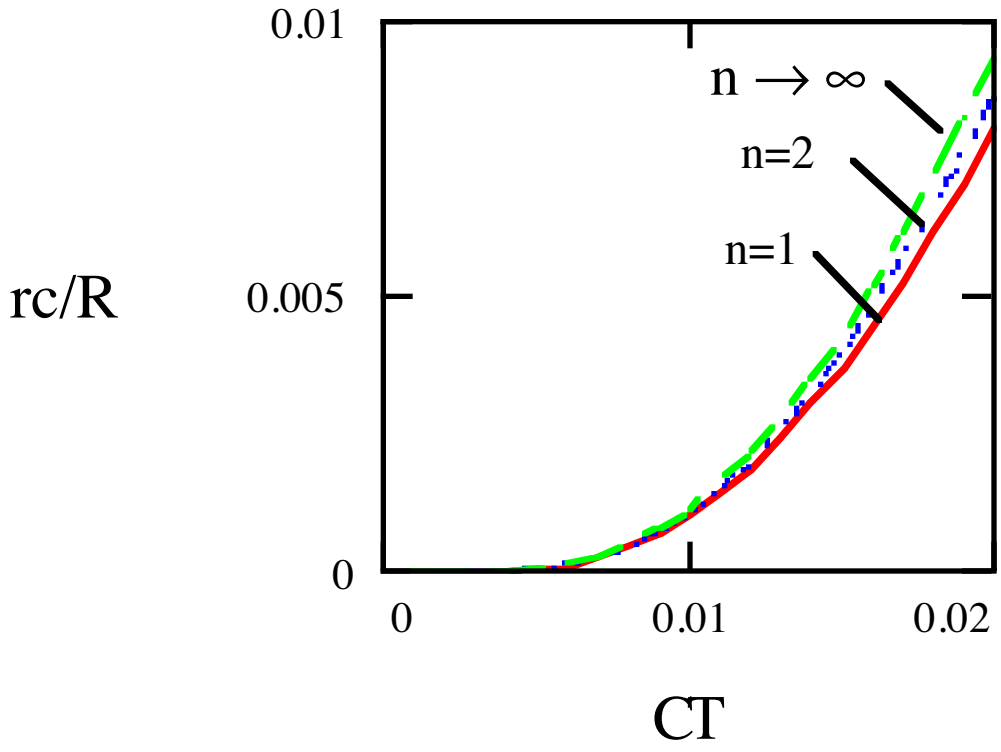

Fig. 5 - Influence Vortex Structure on Core Size for Hovering Rotors (n=1 - Scully model; n=2 - Bagai-Leishman; $n \to \infty$ - Rankine; Eqs. 7, 17a-b, and k=1)

Parametric Assessment

The influence of the induced power constant, k -- which empirically accounts for induced power losses due to the nonuniformity of the rotor wake, blade count, and other factors – is shown in Fig. 6. As can be seen in Fig. 6, rotor induced power, as represented by k, has a profound influence on the vortex core size prediction. One of the difficulties of correlating vortex core size predictions with the available experimental data is that, with a few exceptions, each data point is for a unique rotor configuration, which correspondingly has a unique (and often unknown) induced power constant, k, associated

with it. Given the wide range of rotor configurations comprising the experimental data for vortex core size trends (Tables 1 and 2) it should not be unreasonable to anticipate a wide range of induced power constants for those rotors. In particular, small-scale rotors with untwisted blades and low tip Reynolds numbers will likely have fairly high induced power constant, k, values, therefore explaining some of the variability in vortex core sizes seen in the experimental results, as demonstrated in Figs. 1, 3, and 4. This issue will need to be studied in further detail in future experimental investigations.

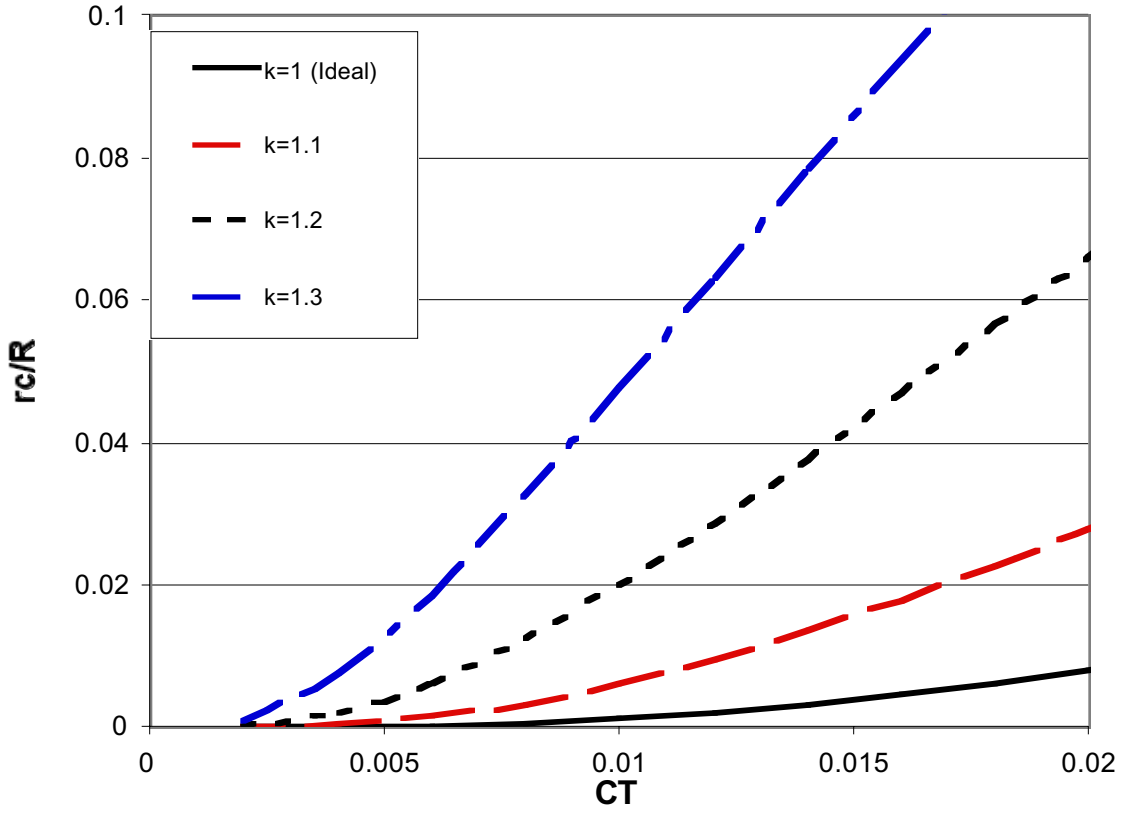

Fig. 6 – Influence of Rotor Induced Power Losses on Rotor Near-Wake Vortex Core Size in Hover

The derived vortex core size expressions, Eqs. 7 and 17a-b, are also applicable to rotor axial flow conditions for small μ_z. Figure 7 shows the predicted trend of vortex core size with C_T and μ_z (assuming, in this case, k=1). Predictions from Eqs. 7 and 17a-b suggest that, for

small μ_z, that as axial-low advance ratio increases, core size decreases. Implicit, though, in the derivation of these vortex core size analytical expressions is the assumption that the rotor disk loading is low and, correspondingly, the trailed vortex filament helical pitch angles are small. Clearly, as axial-flow advance ratios become fairly large this helical pitch angle assumption will at some point become invalid.

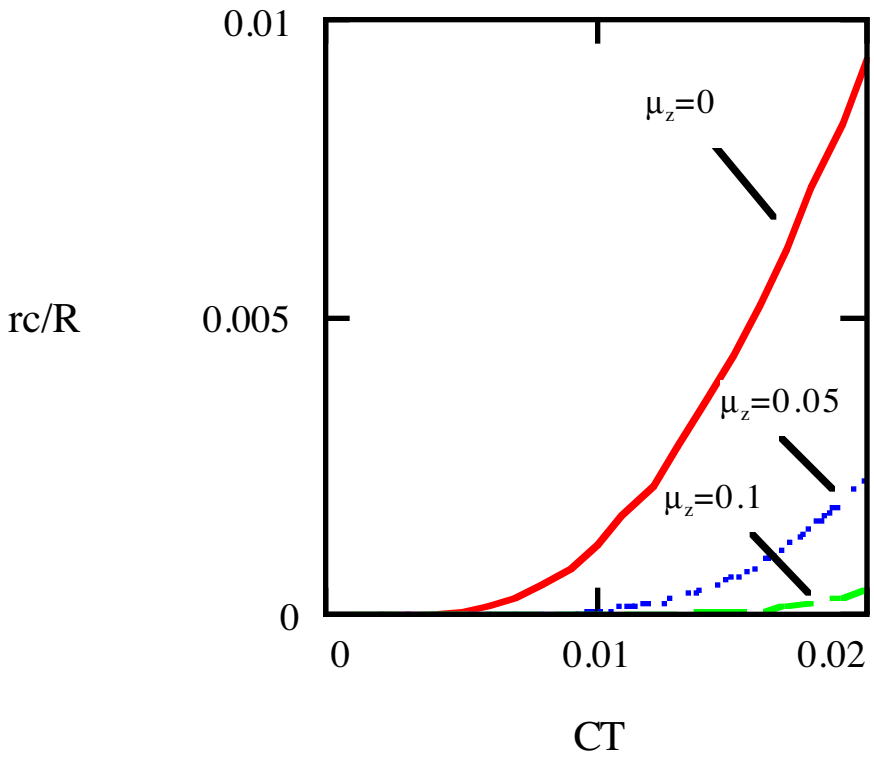

Fig. 7 - Influence of Rotor Disk Loading and Advance Ratio on Vortex Core Size (Eq. 7 and k=1)

Figure 8 summarizes axial-flow vortex core size measurements from the literature. For large values of $C_T/\lambda^2(\mu_z+\lambda)$ there is a significant divergence of the predicted trend as compared to the limited experimental data. It is clear from Fig. 8 that the vortex filament helical pitch angle assumption does indeed break down, and at fairly low advance ratios at that. Further, as previously noted, the high advance ratio vortex core size trend seems to asymptotically

approach r_c/R values of the magnitude estimated (Prandtl, as cited in Ref. 1) for trailed fixed-wing tip vortices.

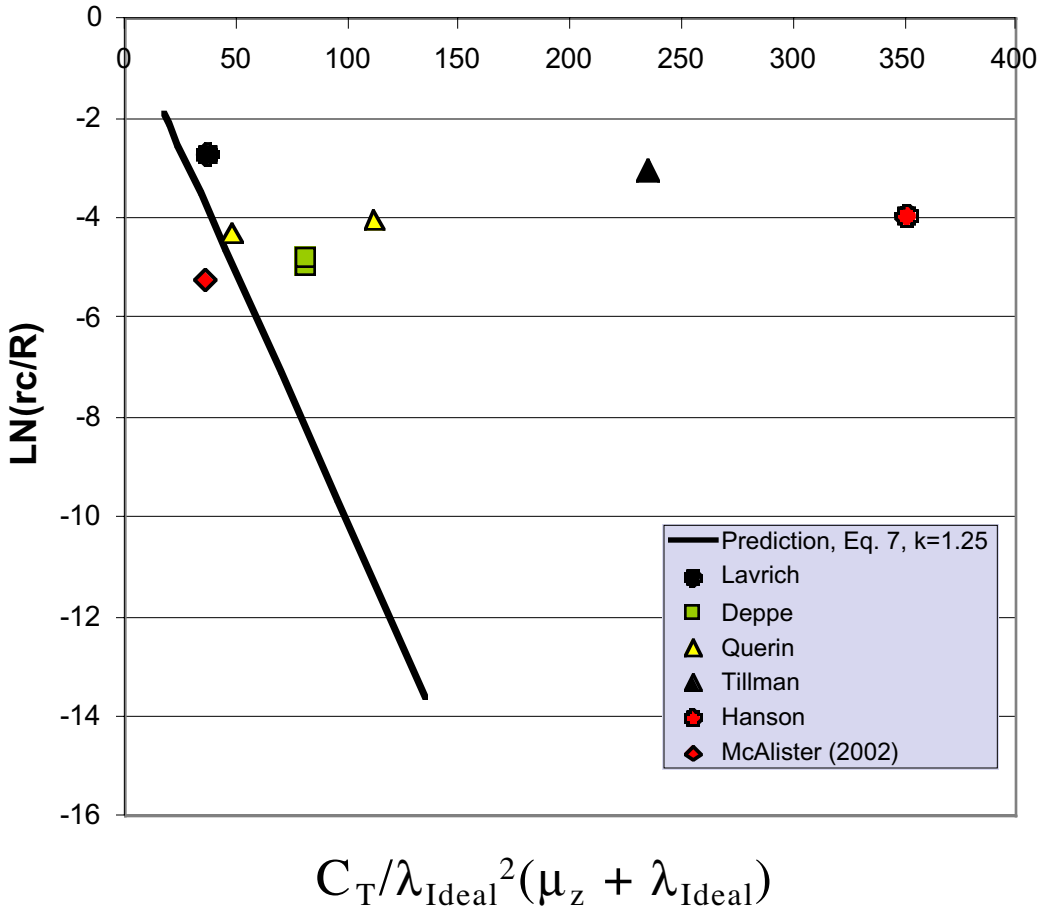

Fig. 8 – Experimental Vortex Core Trends and Comparison with (Eq. 7) Prediction

Figure 8 data suggests an approximation (Eq. 18a-d) that seems to capture the general trend for vortex core size with respect to the complete range of axial-flow advance ratios. The core size estimates from this approximation are shown in Fig. 9.

$$\ln\left(r_c/R\right) \approx \left(a - \frac{1}{4} \cdot \frac{C_T}{\lambda^2\left(\mu_z + \lambda\right)} \right) \cos\varphi + b \sin\varphi$$

where (18a-b)

$$\varphi \equiv \text{atan}\left(\frac{\mu_z + \lambda}{\lambda} \right)$$

And, where assuming a Rankine-type vortex structure, the constants a and b can be found from Eq. 7 and Prandtl's fixed-wing work summarized in Ref. 1.

$$a = \ln 8 - \frac{7}{4}$$

(18c-d)

$$b = 0.171$$

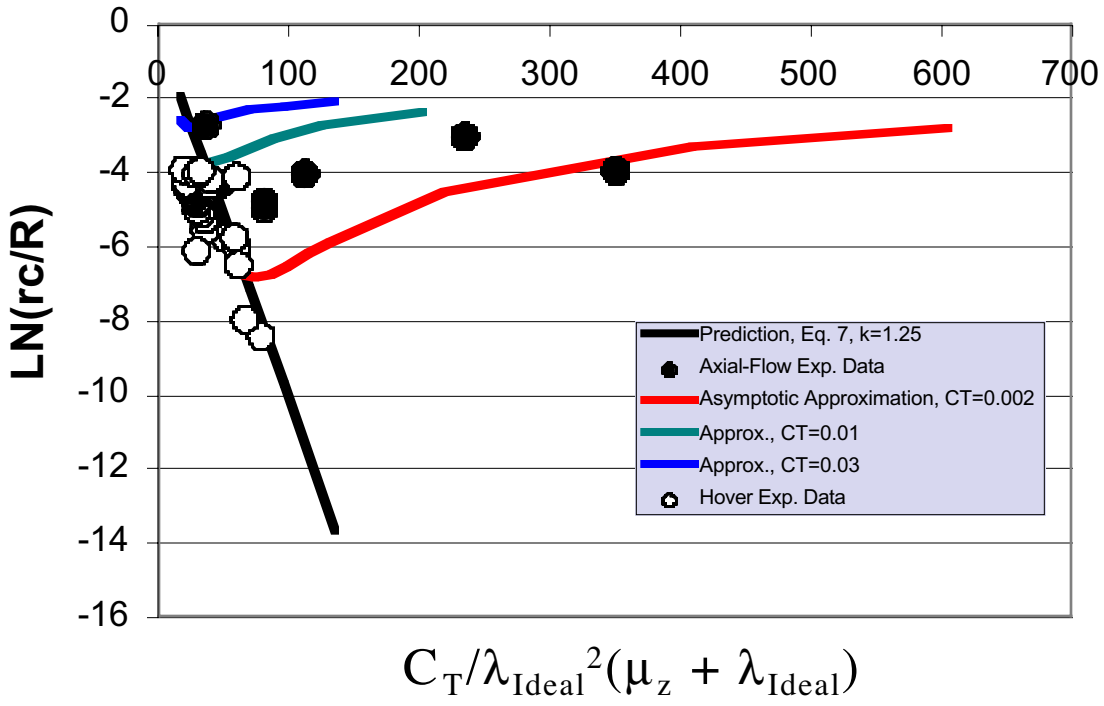

Fig. 9 – An Approximate Relationship for the Complete Axial-Flow Advance Ratio Range

The results from Eq. 18a-d are promising. It is important to stress, though, that Eq. 18a-d is not derived from first principles; it is only an approximation. Further, a more methodical set of experiments targeted to rotor/propeller measurements of vortex core size and overall vortex structure is clearly called for so as to refine the observations and analysis, in part, detailed in this paper.

Conclusions

It is generally recognized that high fidelity modeling of the rotor wake is crucial to the accurate estimation of rotor performance, acoustics, and blade structural loads. The vortical structure and size and strength of the trailed tip vortices from the rotor blades are key considerations for modeling of rotor wakes. A number of empirical and semi-empirical models have been employed to date to define rotor tip vortex core size. In many cases the vortex core size is often adjusted on a trial and error basis in even fairly sophisticated comprehensive rotor analyses models to improve overall rotor prediction correlation with experimental data.

The paper began with a survey of existing literature related to experimental measurements of near-wake (trailed vortices close to the rotor disk, i.e. at early wake ages) rotor vortices in hover and axial-flow flight. The focus of most of the investigations in the literature have been on the development/refinement and demonstration of various experimental techniques employed to image and/or directly measure the rotor vortex velocities and structure. Further, in many cases, the rotor operating conditions are not fully defined, or cited, and must therefore be inferred. Very few individual studies attempted systematic parametric investigations of the effect of rotor characteristics and operating conditions on vortex structure, strength, and core size. However, by compiling data from multiple sources, and with some reasonable inferences/assumptions, a clearer picture of rotor near-wake vortex core size trends was revealed. The chief and foremost observation from this compilation of experimental data from the literature is that vortex core size (scaled relative to the rotor radius) in the near-wake of hovering rotors is indeed a function of rotor thrust and induced power losses. Vortex core size is not, as has been previously suggested, invariant

with thrust (i.e. $r_c/R \approx$ constant, for all C_T), nor is it directly/simply an artifact of rotor blade/tip geometry (i.e. $r_c/c \approx$ constant, for all C_T and R). These obsolete empirical rules stem primarily from experimental investigations of rotors with low disk loading and, in some cases, large induced power losses.

Using a kinetic energy conservation approach, a number of simple analytic expressions were derived for estimating the core size of tip vortices in the near-wake of rotors in hover and axial-flow flight. The influence of thrust, induced power losses, advance ratio, and vortex structure on rotor vortex core size was assessed. The analytical predictions were correlated with the experimental data from the literature. For hovering rotors good agreement was found between the predictions and the experimental trends. For the rotor/propeller axial-flow flight data, not unexpectedly given the analytical modeling assumptions, good agreement existed only for low advance ratios; poor agreement was seen for large advance ratios. An alternate approximate expression was suggested for rotor near-wake vortex core size trends under axial-flow flight conditions. This approximate expression provided substantially improved agreement (over the purely analytic expressions) with the vortex core size data for the complete advance ratio range.

In general, three conclusions can be drawn from the work in this paper. First, the greater the rotor thrust, the larger the vortex core size in the rotor near-wake. Second, the more efficient a rotor, or propeller, is with respect to factors that affect induced power losses, the smaller the resulting vortex core size. Third, and lastly, vortex core size decreases in magnitude from hover values for small axial-flow advance ratios; but, as advance ratio increases to moderate and large values, rotor vortex core size asymptotically increases to a large trailed vortex core size.

References

1. Durand, W.F., *Aerodynamic Theory*, 1934.

2. Saffman, P.G., *Vortex Dynamics,* Cambridge University Press, 1992.

3. Young, L.A., "Rotor Vortex Filaments: Living on the Slipstream's Edge," NASA TM 110431, January 1997.

4. Wadcock, A.J., "Measurement of Vortex Strength and Core Diameter in the Wake of a Hovering Rotor," AHS Technical Specialists' Meeting for Rotorcraft Acoustics and Aerodynamics, Williamsburg, VA, October 28-30, 1997.

5. Ananthan, S., Leishman, J.G., and Ramasamy, M., "The Role of Filament Stretching in the Free-Vortex Modeling of Rotor Wakes," 58th Annual Forum of AHS International, Montreal, CA, June 11-13, 2002.

6. Leishman, J.G., Baker, A., and Coyne, A., "Measurements of Rotor Tip Vortices Using Three-Component Laser Doppler Velocimetry," AHS Aeromechanics Specialist Conference, Fairfield County, CT, October 11-13, 1995.

7. Han, Y.O., Leishman, J.G., Coyne, A.J., "On the Turbulent Structure of a Tip Vortex Generated by a Rotor," American Helicopter Society 52nd Annual Forum, Washington, DC, June 4-6, 1996.

8. Swanson, A. and Light, J., "Shadowgraph Flow Visualization of Isolated Tiltrotor and Rotor/Wing Wakes," American Helicopter Society 48th Annual Forum, Washington, DC, June 3-5, 1992.

9. Thompson, T.L., Komerath, N.M., and Gray, R.B., "Visualization and Measurement of the Tip Vortex Core of a Rotor Blade in Hover," Journal of Aircraft, Vol. 25, No. 12, December 1988.

10. Cook, C.V., "The Structure of the Rotor Blade Tip Vortex," AGARD Conference Proceedings No. 111, Marseilles, France, September 1972.

11. Müller, R.H.G., "Measurement of Helicopter Rotor Tip Vortices Using the 'Flow Visualization Gun'-Technique," Eighteenth European Rotorcraft Forum, Avignon, France, September 15-18, 1992.

12. Pouradier, J.M. and Horowitz, E., "Aerodynamic Study of a Hovering Rotor," Sixth European Rotorcraft and Powered Lift Aircraft Forum, Bristol, England, September 16-19, 1980.

13. Seelhorst, U., Beesten, B.M.J., and Bütefisch, K.A., "Flow Field Investigation of a Rotating Helicopter Rotor Blade by Three-Component Laser-Doppler-Velocimetry," AGARD Symposium on Aerodynamics and Aeroacoustics of Rotorcraft, AGARD # CP-552, Berlin, Germany, October 10-14, 1994.

14. Heineck, J.T., Yamauchi, G.K., Wadcock, A.J., and Lourenco, L., "Application of Three-Component PIV to a Hovering Rotor Wake," 56th Annual Forum of the American Helicopter Society, Virginia Beach, VA, May 2-4, 2000.

15. Martin, P.B. Pugliese, G.J., and Leishman, J.G., "High Resolution Trailing Vortex Measurements in the Wake of a Hovering Rotor," 57th Annual Forum of the AHS International, Washington, DC, May 9-11, 2001.

16. Martin, P.B. and Leishman, J.G., "Trailing Vortex Measurements in the Wake of a Hovering Rotor Blade With Various Tip Shapes," 58th Annual Forum of the AHS International, Montreal, Canada, June 11-13, 2002.

17. University of Maryland, Department of Aerospace Engineering, "Studies of Rotor Wakes in Hover and Low Speed Forward Flight Using Wide-Field Shadowgraphy," Report # UM-AERO-92-12, College Park, Maryland, 1992.

18. McAlister, K.W., Tung, C., and Heineck, J.T., "Forced Diffusion of Trailing Vorticity from a Hovering Rotor," 57th Annual Forum of AHS International, Washington, DC, May 9-11, 2001.

19. Lavrich, P.L., McCormick, D.C., and Parzych, D.J., "Vortex Structure of Wakes Behind an Advanced Propeller at Takeoff Load Conditions," 13th AIAA Aeroacoustics Conference, AIAA Paper # 90-3978, Tallahassee, FL, October 22-24, 1990.

20. Deppe, L. and Wagner, W.J., "Experimental Investigation of the Periodical Wake Structure of a Wind Turbine Model," Garmisch-Partenkirchen, Federal Republic of Germany, September 22-25, 1986.

21. Querin, O.M., "Flow Visualization of a Small Diameter Rotor Operating at High Rotational Speeds With Blades at Small Pitch Angles," AHS International Specialists' Meeting on Rotorcraft Basic Research, Atlanta, GA, March 1991.

22. Hanson, D.B and Patrick, W.P., "Near Wakes of Advanced Turbopropellers," 12th AIAA Aeroacoustics Conference, AIAA-89-1095, San Antonio, TX, April 10-12, 1989.

23. Tillman, T.G., Simonich, J.C., and Wagner, J.H., "Hot Wire Measurements Downstream of a Prop-Fan," AIAA/ASME/SAE/ASEE 25th Joint Propulsion Conference, Monterey, CA, July 10-12, 1989.

24. McAlister, K.W. and Heineck, J.T., "Measurements of the Early Development of Trailing Vorticity from a Rotor," NASA TP-2002-211848 and AFDD TR-02-A-001, July 2002.

25. Mahalingam, R., Wong, O., and Komerath, N., "Experiments on the Origin of Tip Vortices," AIAA CP 2000-0278.

26. Lamb, H., *Hydrodynamics, Sixth Edition,* Dover Publications, New York, 1945.

27. Stepniewski, W.Z., "Rotary-Wing Aerodynamics: Volume I - Basic Theories of Rotor Aerodynamics (With Application to Helicopters)," NASA CR 3082, January 1979.

28. Johnson, W.J., *Helicopter Theory,* Princeton University Press, 1980.